

Cross Sections for Medium Energy He ions Scattered from Hf and Au Atoms

T. Nishimura¹, K. Mitsuhashi², A. Visikovskiy², and Y. Kido²

1) *Research Center of Ion Beam Technology and College of Engineering, Hosei University, Koganei, Tokyo 184-8584, Japan*

2) *Department of Physics, Ritsumeikan University, Kusatsu, Shiga-ken 525-8577, Japan*

Abstract

The elastic scattering cross sections for medium energy He ions incident on Ni, Hf and Au atoms were measured precisely using a toroidal electrostatic analyzer. We prepared the targets of Ni(~1 nm)/HfO₂(1.5 nm)/Si(001) and Ni(~1 nm)/Au(~0.5 nm)/Si(111) and performed *in situ* ion scattering measurement under ultrahigh vacuum condition. The absolute amounts of Ni, Hf and Au were determined by Rutherford backscattering using 1.5 MeV He ions at a scattering angle of 150°. The scattering cross sections for Hf and Au were normalized by those for Ni to avoid the ambiguities of the number of incident particles, solid angle subtended by a detector, detection efficiency and the He⁺ fractions for the emerging He ions from the surfaces. The results obtained are compared with the simple Lee-Hart formula and the calculated values using the Molière and ZBL potentials and the potentials derived from the Hartree-Fock-Slater wave functions.

I. INTRODUCTION

Medium energy ion scattering (MEIS) spectrometry provides a powerful tool to analyze surface and interface structures[1-6]. In order to determine the absolute amounts of subsurface atomic species such as adsorbates, nano-clusters and reconstructed components of single crystal surfaces, it is essential to employ exact scattering cross sections, which are calculated from inter-atomic potentials. In the low and medium energy regimes, the screening of a nuclear charge by bound electrons becomes pronounced. So far, some screened Coulomb potentials were proposed in an analytic form such as Molière[7] and ZBL (Ziegler-Biersack-Littmark)[8]. The latter is an improved version of the former in low and medium energy regimes. The best way to obtain exact inter-atomic potentials is to solve the Poisson equations based on the Hartree-Fock-Slater atomic model. Hereafter, this is denoted by an HF potential. In this study, however, we calculated the scattering cross sections by simulating the He ion trajectories using the electron distributions derived from the Hartree-Fock-Slater

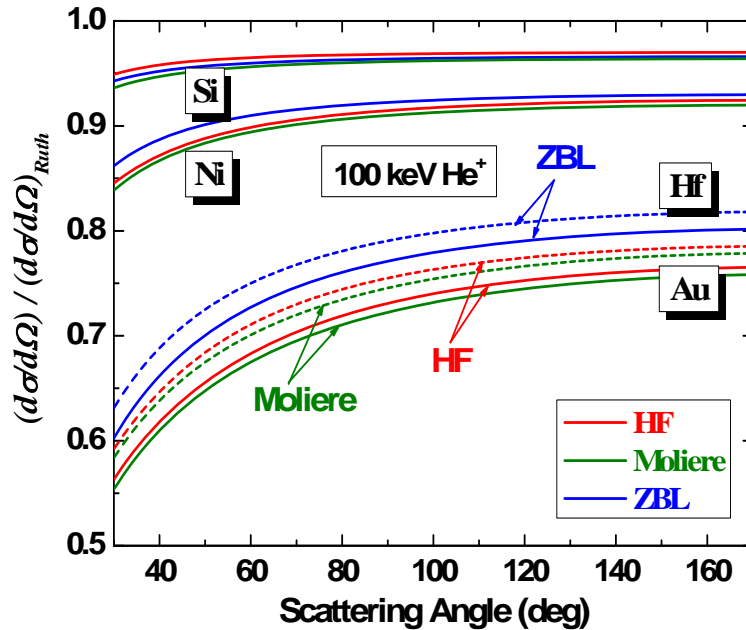


Fig. 1. Cross sections normalized by those calculated from unscreened Coulomb potentials (Rutherford scattering cross sections) for 100 keV He^+ ions scattered from Si, Ni, Hf (dashed curves) and Au atoms, as a function of scattering angle.

wave functions with a spherical symmetry. Figure 1 indicates the scattering cross sections normalized by those calculated from the unscreened Coulomb potentials for 100 keV He⁺ ions scattered from Si, Ni, Hf and Au as a function of scattering angle. With increasing the Z-number, the scattering cross sections calculated from the ZBL potentials deviate pronouncedly from the scattering cross sections calculated from the HF potentials, while the Molière potentials give slight underestimates. Unfortunately, however, the validity of the screened Coulomb potentials has not been evaluated quantitatively in particular for heavy atomic species.

In this study, we measured precisely the elastic scattering cross sections for medium energy He⁺ ions incident on Hf and Au atoms with a toroidal electrostatic analyzer ESA. A problem arises in evaluating the He⁺ fractions, which depend on emerging energy, emerging angle and surface materials[9-11]. In order to avoid this difficulty, we prepared the targets of Ni(0.83 nm)/HfO₂(1.52 nm)/Si(001) and Ni(1.01 nm)/Au(0.40 nm)/Si(111) and performed *in situ* ion scattering measurements under ultrahigh vacuum (UHV) conditions ($\sim 2 \times 10^{-10}$ Torr). The absolute amounts of the Ni, Hf and Au were determined *ex situ* using 1.5 MeV He⁺ ions at a scattering angle of 150°. How to derive the precise scattering cross sections is described later in detail.

II. EXPERIMENT

The MEIS measurement together with Ni and Au depositions were performed *in situ* at Beamline-8 named SORIS working at Ritsumeikan SR Center. The HfO₂ layers were grown on Si(001) substrates by atomic layer deposition. The substrate was annealed at 300°C for 5 min in UHV to eliminate surface contaminations and then cooled down to room temperature (RT) during Ni deposition by a Knudsen cell. Another sample was prepared by Au deposition on sputtered Si(111) substrates followed by Ni deposition at RT. The deposition rates for Ni and Au were 0.87×10^{15} and 0.23×10^{15} atoms/(cm² min), respectively. Both Ni and Au layers were polycrystalline, confirmed by reflection high energy electron diffraction. The samples were transferred

into a scattering chamber and MEIS measurements were performed *in situ* using the toroidal ESA (three-stage micro-channel plates (MCP) combined with a semiconductor position sensitive detector) mounted on a turn table. In order to suppress sputter erosion by He^+ impact, we shifted slightly the beam position on the target after irradiation of an integrated beam current of $1.0 \mu\text{C}$. Indeed, we confirmed that ~ 0.01 ML (~ 0.002 nm) (1 ML: 1.86×10^{15} atoms/cm² for Ni(111)) was sputtered off from the surfaces after irradiation of $1 \mu\text{C}$ for 120 keV He^+ beams. In order to measure the beam current precisely, the sample was positively biased at 90 V for suppression of secondary electron emission.

After the MEIS measurements, RBS analysis was performed *ex situ* at Research Center of Ion Beam Technology of Hosei University using 1.5 MeV He^+ ions. The samples mounted on a 3-axis goniometer was rotated slowly keeping an incident angle of 7° off from the surface normal and a scattering angle of 150° . Figures 2(a) and (b) show typical RBS spectra observed and best-fitted for Ni/HfO₂/Si(001) and Ni/Au/Si(111). The absolute amounts of Ni, Hf and Au were derived by normalizing the simulated spectrum height for the scattering component from the Si substrates to the observed one. We made two corrections on the effects of channeling/blocking dips

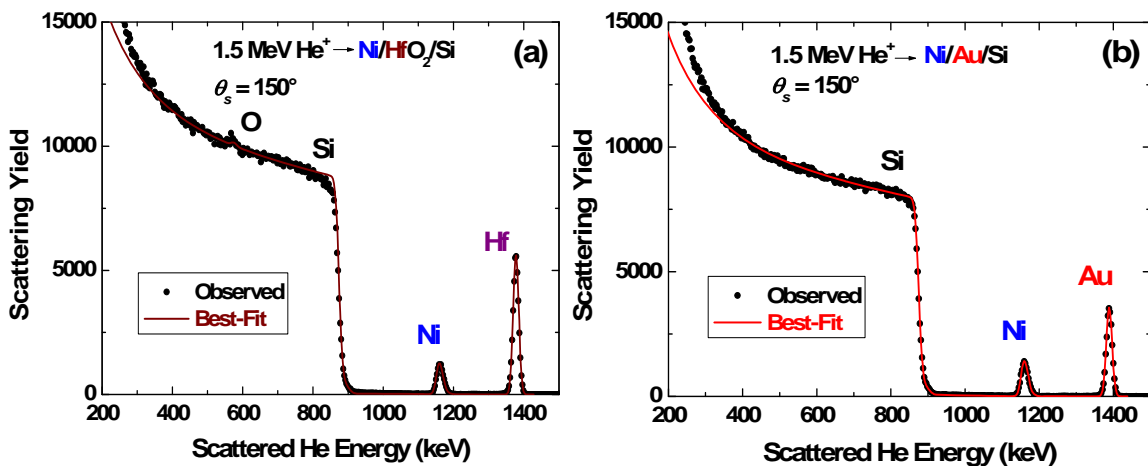


Fig. 2. Energy spectra observed for 1.5 MeV He^+ ions incident on (a) Ni/HfO₂/Si(001) and (b) Ni/Au/Si(111) and scattered at angle of 150° . Solid curves are the best-fitted spectra assuming Ni(0.83 nm)/HfO₂(1.52 nm)/Si(001) and Ni(1.01 nm)/Au(0.40 nm)/Si(111), respectively.

and focusing peaks for the scattering component from the substrates Si deviating from perfect random spectra and of screening of the nuclear charges by bound electrons for Hf and Au atoms (negligibly small for Ni and Si). The screened Coulomb potentials derived from the Hartree-Fock-Slater atomic wave functions[12,13] (a spherical symmetry was assumed for the electron density distributions) reduced the scattering cross sections by 1 - 2% compared with those calculated from the unscreened Coulomb potentials. The former correction of the shadowing focusing effects was made in such a way that the scattering yield from the Si substrate appropriately windowed was measured for the sample rotated slowly around the axis of the surface normal at a fixed incident and scattering angles of 7° and 150° from the axis, respectively. This correction led to increase in the spectrum height of 5-8 %. These corrections kept a good accuracy of the RBS analysis. The other factor affecting the spectrum height comes from the stopping power of Si dependent on He energy. We employed the stopping powers of Si given by Ziegler et al.[14]. Fortunately, however, as explained later, the relative amount of Hf(Au) to Ni appears in the derivation of the scattering cross sections (eq. (3)). Therefore, the uncertainty of the stopping powers of Si does not degrade the accuracy in the present analysis. The sputter etching and mixing effects induced by He^+ -ion irradiation are also negligibly small because of the high impact energy of 1.5 MeV and of shifting the irradiation area by sample rotation. It is, of course, essential to obtain good statistics in the scattering yields. The total yields acquired for Ni, Hf and Au are over 10000 counts, which led to a statistical error below $\sim 1\%$. As the results, the uncertainty of $\sim 2\%$ at most is expected for the relative thickness of Ni/Hf(Au), which appears in the derivation of the scattering cross sections (see eq. (3)). The absolute amounts of Ni, Hf and Au were determined by making the simulated total scattering yields coincident with the observed ones after background subtraction from the dark currents of the solid state detector employed.

III. DATA ANALYSIS

The scattering yield Y_{Ni} (count/ μC) from Ni atoms of Ni/HfO₂/Si(001) (Ni/Au/Si(111)) detected by the toroidal ESA is expressed by

$$Y_{Ni} = Q \left(\frac{d\sigma}{d\Omega} \right)_{Ni}^{HF} (N\Delta x)_{Ni} \Delta\Omega \cdot \varepsilon \cdot \eta_+, \quad (1)$$

where $Q = 0.624 \times 10^{13}$ (= 1 μC), $\left(\frac{d\sigma}{d\Omega} \right)_{Ni}^{HF}$ scattering cross section for Ni atom calculated from the HF potential and $(N\Delta x)_{Ni}$ amount of Ni coverage determined by the RBS measurement. In the previous study[14], we confirmed that the HF potential reproduced well the scattering yields for medium energy He ions incident on polycrystalline Ni layers grown on slightly oxidized Si(111) substrates using a solid state detector. The solid angle subtended by the toroidal ESA, the detection efficiency and the He⁺ fraction for He ions emerging from Ni surfaces are denoted by $\Delta\Omega$ (0.764×10^{-4}), ε (0.44) and η_+ , respectively. The detection efficiency ε is assumed to be constant for impinging He⁺ and neutrals in the energy range from 1 to 100 keV[15], while η_+ depends on emerging angle and energy. The above detection efficiency was measured at incident He energy of ~80 keV by a surface barrier solid state detector using a thin Au layer deposited on a slightly oxidized Si(111) substrate. The scattering yield observed for Hf (Au) atoms of the same sample is given by

$$Y_{Hf} = Q \left(\frac{d\sigma}{d\Omega} \right)_{Hf} (N\Delta x)_{Hf} \Delta\Omega \cdot \varepsilon \cdot \eta_+', \quad (2)$$

where $\left(\frac{d\sigma}{d\Omega} \right)_{Hf}$ is the scattering cross section for Hf (Au) target to be determined and $(N\Delta x)_{Hf}$ is the amount of Hf atoms given by the RBS measurement. Coupling the above two relations, we obtain the scattering cross section of interest given by

$$\left(\frac{d\sigma}{d\Omega} \right)_{Hf} = \frac{Y_{Hf}}{Y_{Ni}} \cdot \frac{(N\Delta x)_{Ni}}{(N\Delta x)_{Hf}} \cdot \frac{\eta_+}{\eta_+'} \cdot \left(\frac{d\sigma}{d\Omega} \right)_{Ni}^{HF}. \quad (3)$$

Here, we must note that η_+' is slightly different from η_+ because of slightly different emerging energy. The η_+' values was estimated to be $\eta_+ + \Delta\eta_+$, where $\Delta\eta_+$ was

derived from the emerging energy dependent η_+ measured previously for polycrystalline Ni films[11]. The η_+/η'_+ value ranges from 0.94 to 0.96 and the uncertainty is probably less than 0.5 %. In order to suppress the effect of non-equilibrium charge fractions, we set a large emerging angle of 60° with respect to surface normal. Actually, this correction is negligibly small, because of cancelation of η_+ and η'_+ in the relation (3). Importantly, the other factors of the number of He^+ incidence, the solid angle subtended by the toroidal ESA and detection efficiency do not contribute to the derivation of the scattering cross sections, as seen from the relation (3). In the quite same manner, the scattering cross sections for the Au target are also determined.

IV. RESULTS AND DISCUSSION

Figures 3(a) and (b) show typical MEIS spectra observed for 120 keV He^+ ions scattered from Ni(0.83 nm)/HfO₂(1.52 nm)/Si(001) and Ni(1.01 nm)/Au(0.40 nm)/Si(111), respectively. The vertical arrows indicate the emerging energy positions if the Ni, Hf and Au layers are located on top of the surfaces. The MEIS spectra reveal that the Ni/HfO₂/Si has a good uniformity, whereas Ni and Au are slightly interdiffused at the Ni/Au and Au/Si interfaces. However, such nonuniformity of the Ni and Au layers does not affect the measurement of the scattering cross sections.

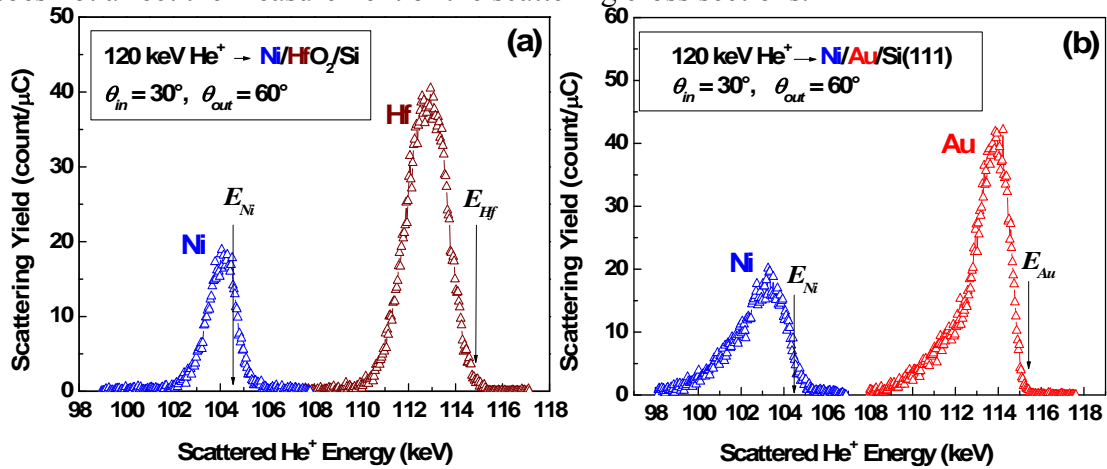


Fig. 3. MEIS spectra observed for 120 keV He^+ ions scattered from (a) Ni/HfO₂/Si(001) and (b) Ni/Au/Si(111) at incident and emerging angles of 30° and 60° , respectively. Vertical arrows indicate the emerging energies of He ions scattered from Ni, Hf and Au located on top of the surfaces.

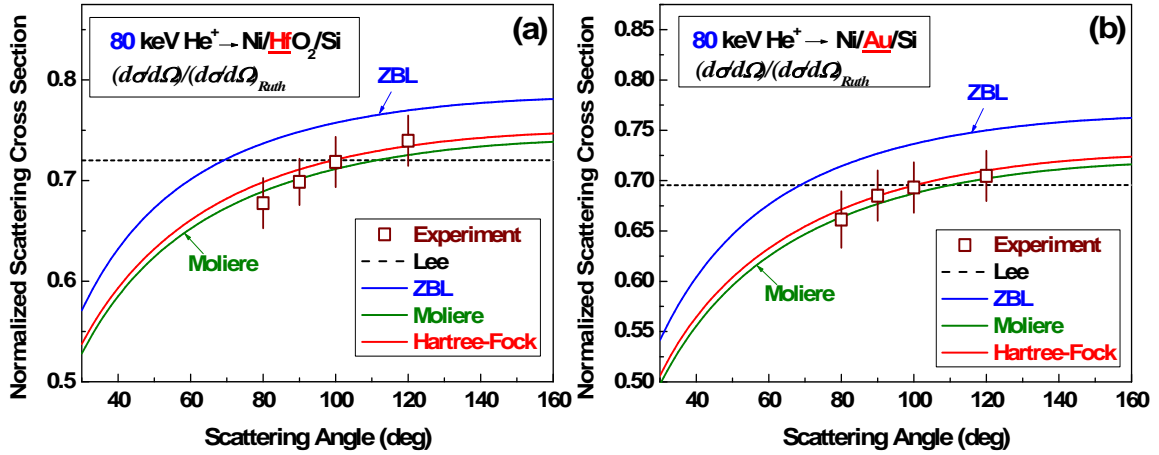


Fig. 4. Normalized cross sections for 80 keV He^+ ions scattered from (a) Hf and (b) Au, as a function of scattering angle at fixed emerging angle of 60° . The straight lines drawn are the cross sections given by Lee-Hart formula.

The cross sections normalized by the Rutherford cross sections for 80 keV He^+ ions scattered from Hf and Au are shown as a function of scattering angle in Figs. 4(a) and (b), respectively. We evaluated the uncertainties for the normalized scattering cross sections by repeating the MEIS measurements three times for different two samples and the data points correspond to the mean values. The uncertainties indicated by the error bars do not contradict with the accuracies for the relative thickness of Ni/Hf(Au) determined by RBS and for the relative scattering yield from Ni and Hf(Au) in the relation (3). Indeed, the statistical uncertainties for the scattering yields for Ni, Hf and Au were $\sim 1\%$ in the present MEIS measurement. The observed scattering cross sections for Hf and Au agree well with those calculated from the Molière and HF potentials, while the ZBL potentials lead to considerable overestimates. The straight lines (dashed) drawn in the figures correspond to the normalized scattering cross sections given by the simple formula proposed by Lee and Hart[16]. Obviously the Lee-Hart formula is not applicable to scattering angle below 80° for both Hf and Au. Similar trend is also seen for 120 keV He^+ incidence, as shown in Figs. 5(a) and (b). The ZBL potentials still give overestimates for both Hf and Au, while the Molière potentials result in agreement with the observed scattering cross sections for Hf and Au, although slightly underestimate for Au. Finally, we show the scattering cross sections

for Hf and Au, respectively at a scattering angle of 90° , as a function of incident energy in Figs. 6(a) and (b). The observed scattering cross sections are consistent with those calculated from the Molière and HF potentials, whereas the ZBL potentials lead to overestimates in the whole range from 60 to 140 keV. The simple Lee-Hart formula gives slight overestimates but the deviations from the observed cross sections are below 5 % at most. As pointed out previously, the Lee-Hart formula is applicable to scattering angle above 80° in the medium energy regime. All the data mentioned above are derived assuming the detection efficiency independent of impinging He energy. According to the report of Thompson and Hart[18], the detection efficiency of MCP

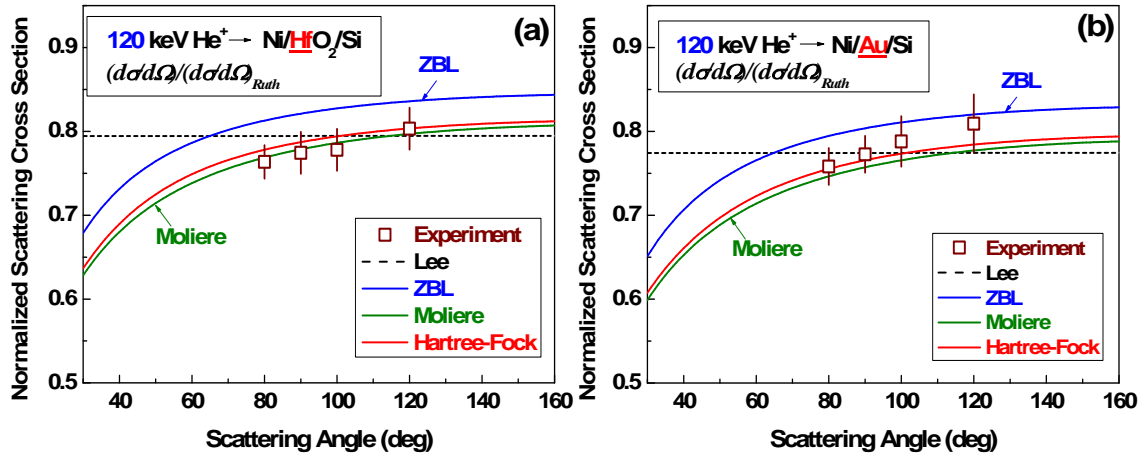


Fig. 5. Normalized cross sections for 120 keV He^+ ions scattered from (a) Hf and (b) Au, as a function of scattering angle at fixed emerging angle of 60° . The straight lines drawn are the cross sections given by Lee-Hart formula.

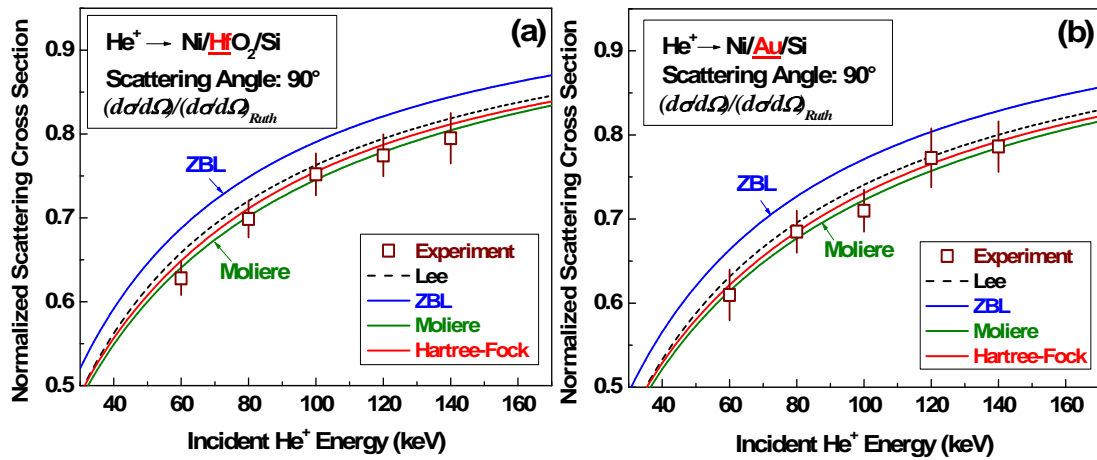


Fig. 6. Normalized cross sections for He^+ ions scattered from (a) Hf and (b) Au at fixed scattering angle of 90° , as a function of incident energy.

depends significantly on ion species and ion energy. We calculated the scattering cross sections assuming the detection efficiencies linearly increasing with incident He energy. However, as can be seen from eq. (3), the corrections are small enough $\sim 1.5\%$ at most.

Finally, some attention is paid to the shadowing effect upon the scattering cross sections, because the shadow cone becomes larger with decreasing the incident He^+ energy. As mentioned before, the HfO_2 layer was amorphous and the Ni and Au were polycrystalline, probably consisting of small domains with c-axis oriented ([111]-axis). It is, of course, very difficult to reproduce an actual scattering process by computer simulations. Despite that, we performed Monte Carlo simulations of He ion trajectories for Ni(111) with five atomic-layer height epitaxially grown on single crystal Au(111) with two atomic-layers to calculate the hitting probabilities dependent on temperature (average thermal lattice vibrations were estimated from the Debye model). Figure 7 shows the hitting probabilities for each atomic-layer atoms as a function of temperature. At a temperature of 20000 K, the one-dimensional mean thermal

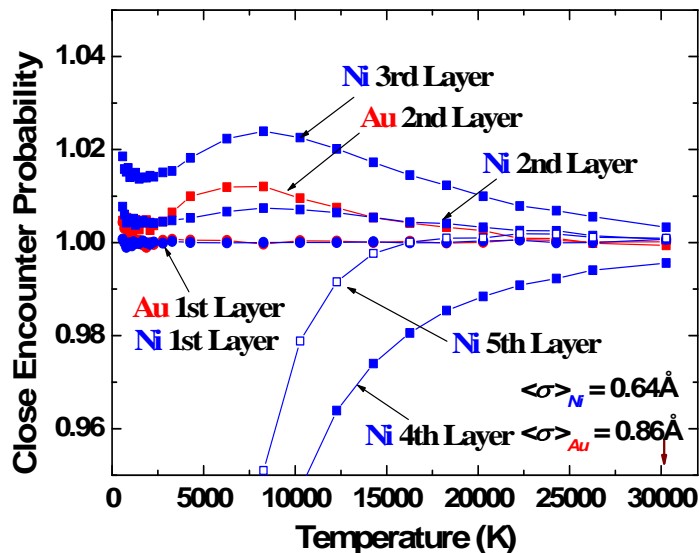


Fig. 7. Close encounter (hitting) probabilities for each layer of Ni and Au atoms as a function of temperature, which were calculated from Monte Carlo simulations assuming 60 keV He^+ ions incident along the [111]-axis of Ni(111) with five atomic-layer height grown epitaxially on single crystal Au(111) with two atomic-layers.

vibration amplitudes for Ni and Au are deduced to be 0.052 and 0.070 nm, respectively, whose displacements correspond to 21 and 24 % of the Ni-Ni and Au-Au bond lengths. All the hitting probabilities at this temperature are almost unity within 0.012. The hitting probabilities more than and less than unity, respectively indicate the experience of the focusing and shadowing effects for the scattered He ions. These two effects counteract each other. From the results mentioned above, it is reasonable that the shadowing and focusing effects do not contribute significantly to the scattering yields for Ni and Au (Hf) in the present MEIS spectra.

V. SUMMARY

The elastic scattering cross sections were measured precisely for medium energy He ions incident on heavy elements of Hf and Au. The targets prepared were Ni(~1 nm)/HfO₂(1.5 nm)/Si(001) and Ni(~1 nm)/Au(~0.5 nm)/Si(111), whose absolute thickness was determined in advance by Rutherford backscattering using 1.5 MeV He⁺ ions. The presence of the topping Ni layers reduced remarkably the uncertainty for the He⁺ fractions dependent on emerging energy and surface materials. In addition, taking the scattering yield for Hf(Au) relative to that for Ni made the derivation of the scattering cross sections free from the number of He⁺ incidence, the solid angle subtended by the detector and detection efficiency. The observed scattering cross sections agree well with those calculated from the HF potentials, as expected. Interestingly, the Molière potentials give overall agreement with the present results, while the ZBL potentials lead to overestimates for both Hf and Au. It is also shown that the simple Lee-Hart formula is applicable to scattering angle above 80° within deviations less than 3 – 5 %.

Acknowledgments

The authors are grateful to Dr. K. Iwamoto for preparing HfO₂ sample. Thanks

are also due to H. Okumura, F. Matsuda and M. Tagami for their help in the MEIS measurements.

References

- [1] J.F. van der Veen, *Surf. Sci. Reports* **5** (1985) 199.
- [2] M. Copel and R.M. Tromp, *Phys. Rev. Lett.* **72** (1994) 1236.
- [3] K. Kimura, K. Ohshima and M. Mannami, *Appl. Phys. Lett.* **64** (1994) 2232.
- [4] E.P. Gusev, H.C. Lu, T. Gustafsson and E. Garfunkel, *Phys. Rev.* **B 52** (1995) 1759
- [5] T. Nishimura, A. Ikeda, H. Namba, T. Morishita and Y. Kido, *Surf. Sci.* **421** (1999) 273.
- [6] P. Bailey, T.C.Q. Noakes and D.P. Woodruff, *Surf. Sci.* **426** (1999) 358.
- [7] G. Molière, *Z. Naturforsch.* **A 2** (1947) 133.
- [8] J.F. Ziegler, J.P. Biersack and W. Littmark, *The Stopping and Range of Ions in Matter* (Pergamon, New York, 1985).
- [9] Y. Kido, T. Nishimura and F. Fukumura, *Phys. Rev. Lett.* **82** (1999) 3352.
- [10] T. Okazawa, K. Shibuya, T. Nishimura and Y. Kido, *Nucl. Instrum. Methods* **B 256** (2007) 1.
- [11] Y. Kitsudo, K. Shibuya, T. Nishimura, Y. Hoshino, I. Vickridge and Y. Kido, *Nucl. Instrum. Methods* **B 267** (2009) 566.
- [12] E. Clementi and C. Roetti, *Atomic Data Nucl. Data Tables* **14** (1974) 177.
- [13] A.D. McLean and R.S. McLean, *Atomic data Nucl. Data Tables* **26** (1981) 197.
- [14] Y. Hoshino and Y. Kido, *Phys. Rev.* **A 68** (2003) 012718.
- [15] K. Tobita, H. Takeuchi, H. Kimura, Y. Kusama and M. Nemoto, *Jpn. J. Appl. Phys.* **26** (1987) 509.
- [16] S.R. Lee and R.R. Hart, *Nucl. Instrum. Methods* **B 79** (1993) 463.
- [17] K.G. Thompson and R.R. Hart, *Nucl. Instrum. Methods* **A 371** (1996) 563.